NASA TECHNICAL MEMORANDUM

NASA TM X-62,435

NASA TM X-62,435

FRACTOGRAPHY OF THE HIGH TEMPERATURE HYDROGEN ATTACK OF A MEDIUM CARBON STEEL

Howard G. Nelson and R. Dale Moorhead

Ames Research Center
Moffett Field, Calif. 94035

May 1975

1. Report No.	2. Government Accession No.	3. Recipient's Catalog No.
TM X-62,435		

4. Title and Subtitle	5. Report Date
Fractography of the High Temperature Hydrogen Attack of a Medium Carbon Steel	6. Performing Organization Code

7. Author(s)	8. Performing Organization Report No.
Howard G. Nelson and R. Dale Moorhead	A-6079
	10. Work Unit No.
9. Performing Organization Name and Address	505-01-21-02-00-21
NASA Ames Research Center Moffett Field, Calif. 94035	11. Contract or Grant No.
	13. Type of Report and Period Covered
12. Sponsoring Agency Name and Address	Technical Memorandum
National Aeronautics and Space Administration Washington, D. C. 20546	14. Sponsoring Agency Code

15. Supplementary Notes

Presented at Symposium on "Fractography-Microscopic Cracking Processes," 78th Annual Meeting of ASTM, Montreal, Canada, June 23-27, 1975

16. Abstract

A systematic study was made of the microscopic fracture processes associated with hydrogen attack of a medium carbon steel in a well-controlled, high-temperature, high-purity hydrogen environment. Exposure to a hydrogen pressure and temperature of 3.5 MN/m^2 and 575° C was found to progressively degrade room temperature tensile properties with increasing exposure time. After 408 hr, the maximum exposure time of this study, yield and ultimate strengths were reduced by more than 40 percent and elongation was reduced to less than 2 percent. Initial fissure formation was found to be associated with manganese rich particles, most probably manganese oxide, aligned in the microstructure during the rolling operation. Fissure growth was found to be associated with a reduction in carbide content of the microstructure and was inhibited by the depletion of carbon. The interior surfaces of sectioned fissures or bubbles exhibit both primary and secondary cracking by intergranular separation. The grain surfaces were not smooth and flat but instead were rough and rounded, suggesting a diffusion-associated separation process. Finally, specimens that were failed at room temperature after exposure to hydrogen were found to exhibit mixed mode fracture having varying amounts of intergranular separation, dimple formation, and cleavage, depending on exposure time.

17. Key Words (Suggested by Author(s))	18. Distribution Statement
Carbon steel Elevated temperature Hydrogen attack Decarburization Tensile properties	Unclassified - Unlimited STAR Category - 26

19. Security Classif. (of this report)	20. Security Classif. (of this page)	21. No. of Pages	22. Price*
Unclassified	Unclassified	18	$3.25

*For sale by the National Technical Information Service, Springfield, Virginia 22151

Introduction

A number of energy-related systems, particularly advanced energy conversion systems such as coal gasifiers, involve the containment of hydrogen at high temperatures and pressures.[1] The extended exposure of some structural steels to such an environment can cause severe degradation of their mechanical properties. Such degradation is termed "hydrogen attack" and is thought to be the combined result of internal decarburization and fissuring. Fortunately for the power industry, the requirement for hydrogen containment at high temperatures and pressures has existed for a number of years in the ammonia and petroleum hydrorefining industries and literature on the subject is quite voluminous. Like most industrial problems, however, the great majority of available data are based on specific service experience and may not be directly applicable to the different operating conditions associated with the power industry. For example, industrial hydrogen environments are far from pure and in most cases of failures associated with hydrogen attack, no attempt has been made to characterize in detail the specific environments in which operating data were obtained; as a result, many observations may reflect the influence of gaseous species other than hydrogen.

A few systematic studies have been performed in controlled hydrogen environments and the phenomenon of hydrogen attack has been at least phenomenologically characterized.[2-7] Briefly, it has been established that hydrogen in atomic or protonic form is absorbed into the steel and diffuses to some location where it can react with carbon to form methane. The result is internal decarburization of the steel which causes a corresponding decrease in strength. The methane molecule, being large, will not readily diffuse away but instead will accumulate at internal interfaces, such as grain boundaries,

with an eventual buildup of large internal pressures. The result is internal fissuring of the steel giving rise to a decrease in strength and ductility.

The objective of the present study was to better understand the microscopic fracture processes associated with hydrogen attack of a plain carbon steel in a well controlled, high-temperature, high-purity hydrogen environment. The fractography of gas-filled fissures and failed tensile specimens was analyzed in detail in an effort to identify; (1) any predominant microstructural defect associated with fissure formation, (2) the prevalent modes of fracture, and (3) the contribution of gas-filled fissures to the overall failure process.

Procedure

The material used in this investigation was commercially produced SAE-AISI 1025 steel sheet, 8×10^{-2}-cm thick which consisted of a microstructure of fine pearlite and ferrite having an ASTM grain size number between 9 and 10. Tensile specimens having a gauge length of 7.62 cm were cut with their long axes perpendicular to the direction of rolling. Prior to environmental exposure, specimen surfaces were polished through 3/0 paper, cleaned in acetone and ethyl alcohol, and air dried.

Environmental exposures were conducted in an all-metal-sealed, stainless steel tubular chamber surrounded by a 40-cm long, resistance-heated, tube furnace. Prior to exposure of the specimens to the test environment, the following procedure was followed. The chamber containing thermocoupled specimens was evacuated to less than 6×10^{-1} N/m^2 (5×10^{-3} torr), charged at room temperature with hydrogen to 3.5 MN/m^2 (500 psig), evacuated, brought up to 300° C, charged with 69 kN/m^2 (10 psig) hydrogen for 16 hr, evacuated, raised to 575° C, and given the final charge of hydrogen to 3.5 MN/m^2 (500 psig). The hydrogen was of laboratory grade that initially contained less than 100 ppm

of active impurity gases (O_2, H_2O, N_2), as determined by mass spectrometric methods; it was additionally purified by passing it slowly through liquid-nitrogen-cooled coils. Specimen temperature was maintained to within ±5° C during environmental exposure. Following exposure, the chamber containing the specimens was evacuated for 30 min while remaining at 575° C and then furnace-cooled. Tensile tests were always conducted at a fixed displacement rate of 1×10^{-2} cm/s within 48 hr after the environmental exposure.

Results and Discussion

A high-purity hydrogen environment at 575° C was found to significantly degrade the tensile properties of SAE-AISI 1025 steel after as few as 136 hr of exposure, the shortest exposure time of this study. These observations are consistent with the operating limits for carbon steel suggested by Nelson[8] based on experience in industrial environments and with published studies of observations made in hydrogen environments.[3-5] Figure 1 is a summary of the tensile curves observed at room temperature after specimen exposure at 575° C to a vacuum environment and a hydrogen environment for various times. Each curve represents an average of two tests. As shown in this figure, yield strength, ultimate strength, and elongation at fracture are all reduced progressively as exposure time is increased. After 408 hr, the maximum exposure time of this study, yield and ultimate strengths are reduced more than 40 percent and elongation is reduced to less than 2 percent.

Figure 2 is a photograph of a portion of a specimen given maximum exposure; as can be seen, severe bubble formation occurred. The larger bubbles were found only on specimens given the maximum hydrogen exposure. These larger bubbles were lenticular, originated some distance below the specimen surfaces, and grew most rapidly parallel to these surfaces. The smaller bubbles, found

on the surfaces of all specimens given hydrogen exposure, were aligned in columns parallel to the rolling direction of the material. These observations suggest that at least at the temperature of this study, initial precipitation occurs at some microstructural feature which has become aligned in the material during the rolling operation. Additionally, the rapid initial formation of the smaller bubbles near the surface, and their lack of continued growth with additional exposure, support the premise that lattice diffusion of the gaseous reaction product is very difficult and that continued growth of near-surface bubbles is inhibited because of depletion of necessary carbon due to surface decarburization; away from the specimen surfaces, sufficient carbon is retained for continued bubble growth.

The initial microstructure of this medium carbon steel was ferrite and fine pearlite. After 136 hr of exposure at 575° C in vacuum, the structure had transformed to spheroidized carbide in a ferrite matrix, and, in hydrogen, the amount of this spheroidized carbide had been significantly reduced. After 248 hr of hydrogen exposure, carbides could not be observed. Figure 3 is a photomicrograph of a specimen given this intermediate hydrogen exposure. As can be seen, the ferritic grain size has remained small, carbides cannot be distinguished, and a number of fissured areas are present. One such fissured area is shown in Fig. 4a at a higher magnification. In this figure, separation along grain boundaries can be seen to envelop what appear to be two particles. Using energy dispersive X-ray analysis, it is seen in Figs. 4b and 4c, which are the images for iron and manganese, respectively, that these particles are not iron but that they contain manganese. Because no sulfur was evident, these inclusions are most probably manganese oxide. A great number of such fissured areas were studied in this manner and in every case manganese inclusions were observed to be present. This suggests that initial

precipitation of the gaseous reaction product occurs at the interface of the iron/manganese particles which have been aligned during the rolling operation (Fig. 2). Continued precipitation results in grain boundary separation in the nearby material.

The interior surface of the largest bubble shown in Fig. 2 was examined in an effort to establish the fracture mode associated with massive bubble growth. Figure 5 consists of four SEM micrographs of the interior surface of the sectioned bubble at various magnifications. At the higher magnifications (Figs. 5c and 5d) it is seen that both primary and secondary cracking occurred by intergranular separation. The grain surfaces, however, do not show the flat, smooth facets normally observed with intergranular fracture. Instead, the grains are seen to be somewhat rough and rounded, more typical of the fracture surface of material failed by a diffusion associated creep-rupture mechanism at very high temperatures.[9] For carbon steel, a 575° C exposure temperature is not high compared with true melting temperature of about 1500° C, and thus diffusion associated creep-rupture would not normally be expected. This suggests that an additional influence may be important in addition to the simple mechanical consideration of the formation of a high internal pressure. Carbon, for example, has been shown to increase self-diffusion in alpha-iron by as much as four orders of magnitude.[10] One possibility is that bubble growth may be enhanced at locations where carbon concentrations are high or, alternatively, similar enhancement may be realized as the result of the presence of hydrogen in solution. Certainly, more work is required to understand this observation.

Finally, Fig. 6 is a series of SEM fractographs typical of specimens failed at room temperature after exposure to a vacuum environment (Fig. 6a) and a hydrogen environment (Figs. 6b and 6c). Failure of specimens not

exposed to hydrogen occurred by the normally observed ductile mode of void coalescence with the resulting dimpled surface morphology (Fig. 6a). After hydrogen exposure, a mixed-mode fracture surface, consisting of varying amounts of intergranular separation and dimple formation (Fig. 6b), was observed depending on exposured time. Because of the rounded nature of the grain faces (Fig. 6b), similar to those previously observed (Figs. 5c and 5d), the intergranular portion of the failure most probably occurred during hydrogen exposure. Additionally, scattered areas of what appeared to be cleavage failure (Fig. 6c) were found on the fracture surfaces of the specimens given maximum hydrogen exposure. This latter observation suggests that the strength of the metal lattice may have been affected by the presence of the reaction product.

General Conclusions

Fractographic analysis has proved to be a useful tool in helping to understand the microscopic fracture processes associated with hydrogen attack. Although no previously unresolved questions were answered by this investigation, important points were raised which require study in the future. For example, what role do the manganese-rich particles play in the initial process of fissure formation? Or is diffusion-associated creep-rupture the primary mechanism of fracture in hydrogen environments at elevated temperatures? If so, how does this occur at temperatures which are so far below the melting point of medium carbon steel? Work is being undertaken to address these questions and other important points related to the hydrogen attack of steels.

References

1. Youngblut, K. C., Mat. Protect. and Preform., Vol. 12, 1973, pp. 33-36.
2. Allen, R. E., Jansen, R. J., Rosenthal, P. C., and Vitovec, F. H., Proc. Am. Petrol. Inst., Vol. 41, 1961, pp. 74-84.
3. Allen, R. E., Jansen, R. J., Rosenthal, P. C., and Vitovec, F. H., Proc. Am. Petrol. Inst., Vol. 42, 1962, pp. 452-462.
4. Weiner, L. C., Acta Met., Vol. 8, 1960, pp. 52-53.
5. Weiner, L. C., Corrosion, Vol. 17, 1961, pp. 137t-143t.
6. Vitovec, F. H., Proc. Amer. Petrol. Inst., Vol. 44, 1964, pp. 179-188.
7. Westphal, D. A. and Worzala, F. J., in Hydrogen in Metals, Thompson and Bernstein, Ed., ASM, Metals Park, Ohio, 1974.
8. Nelson, G. A., "Action of Hydrogen on Steel at High Temperature and High Pressure," Welding Research Council Bulletin No. 145, October, 1969.
9. Metals Handbook, Vol. 9, Fractography and Atlas of Fractographs, ASM, Metals Park, 1974, pp. 75-76.
10. Krishtal, M. A., Diffusion Processes in Iron Alloys, Metallurgizdat, Moskva, 1963 (Translated from Russian, Israel Prog. Sci. Translations, Jerusalem, 1970).

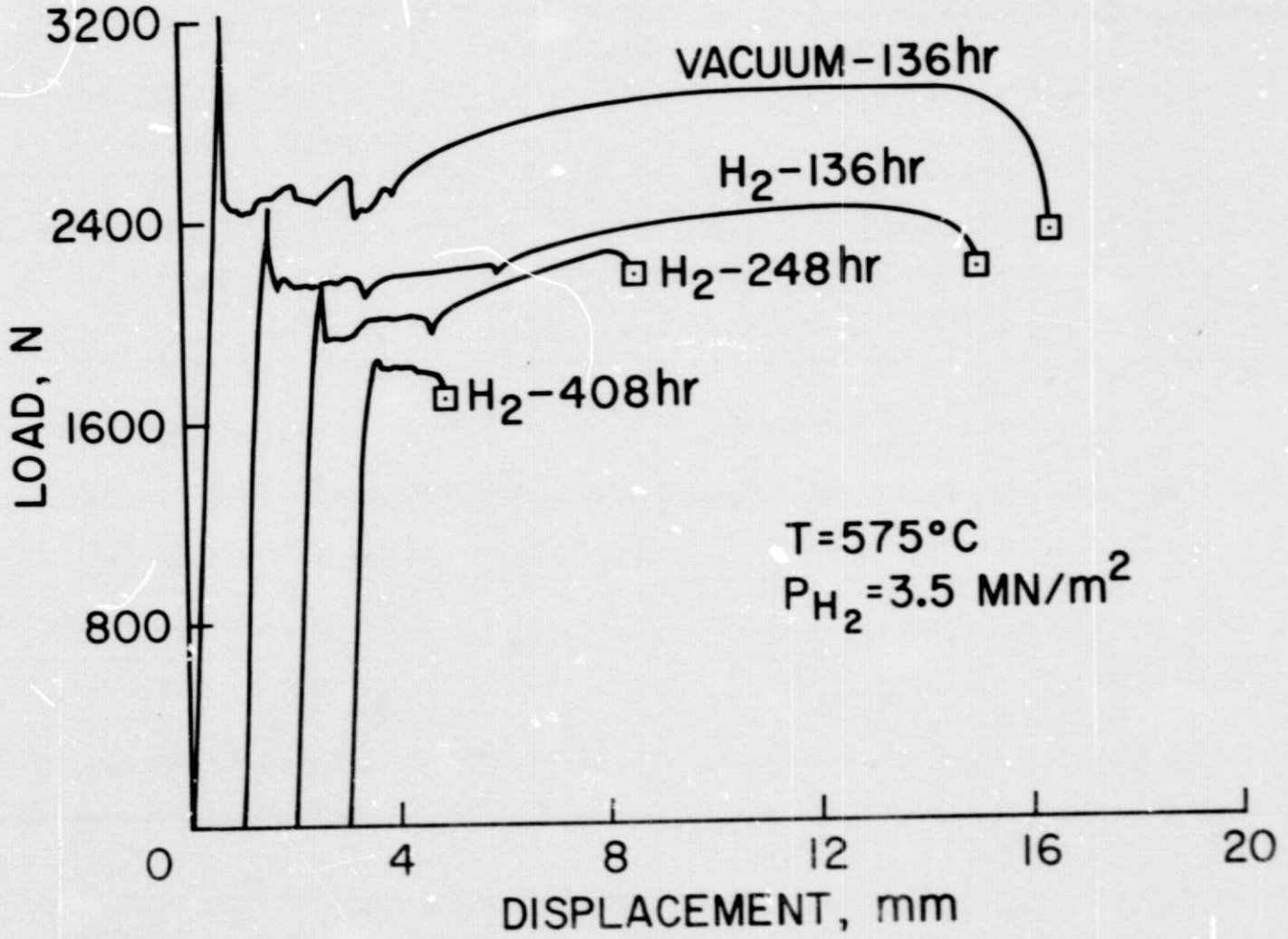

Fig. 1 - A summary of tensile curves observed for 1025 steel after exposure to a vacuum environment and a hydrogen environment for various times at 575° C.

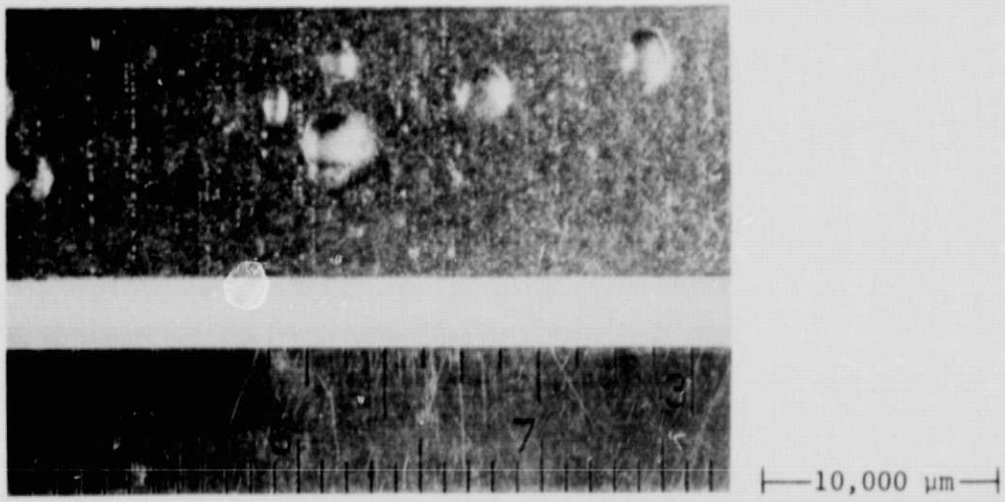

Fig. 2 - A portion of a tensile specimen exposed to 3.5 MN/m² hydrogen at 575° C for 408 hr.

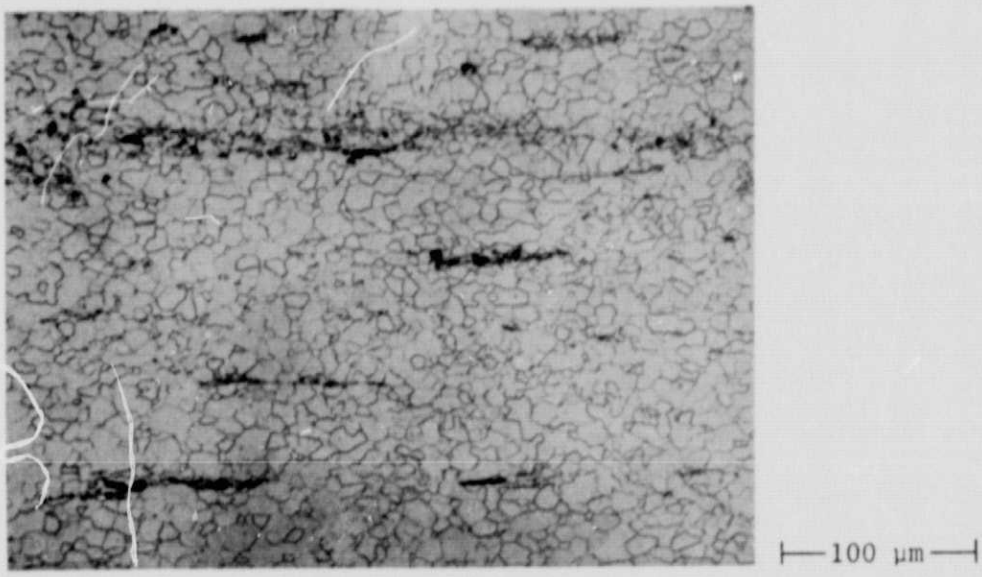

Fig. 3 - The microstructure of a specimen given intermediate hydrogen exposure. Etchant - 3 percent Nital.

(a) *SEM image.*

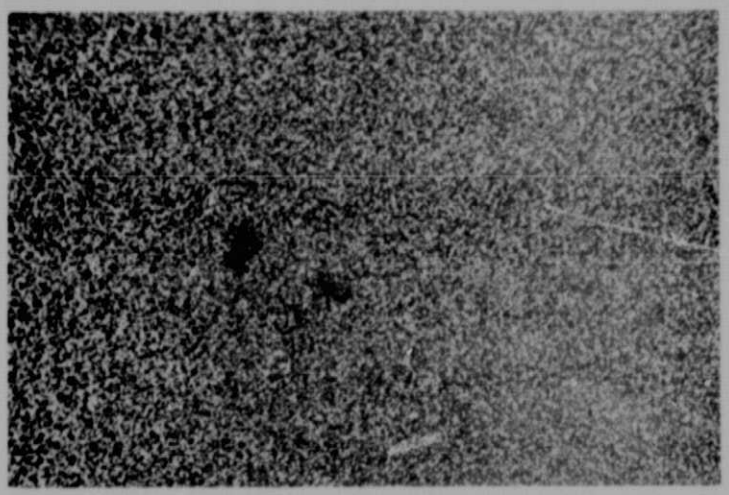

(b) *Iron image using energy dispersive X-ray analysis.*

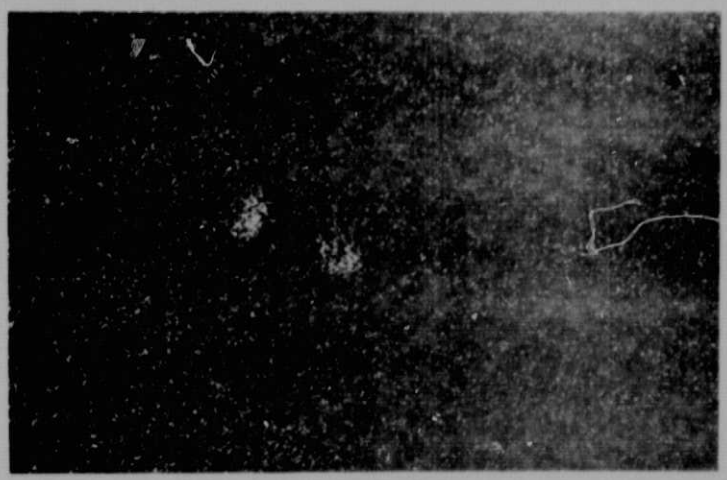

(c) *Manganese image using energy dispersive X-ray analysis.*

Fig. 4 - A typical fissured area shown in Fig. 3.

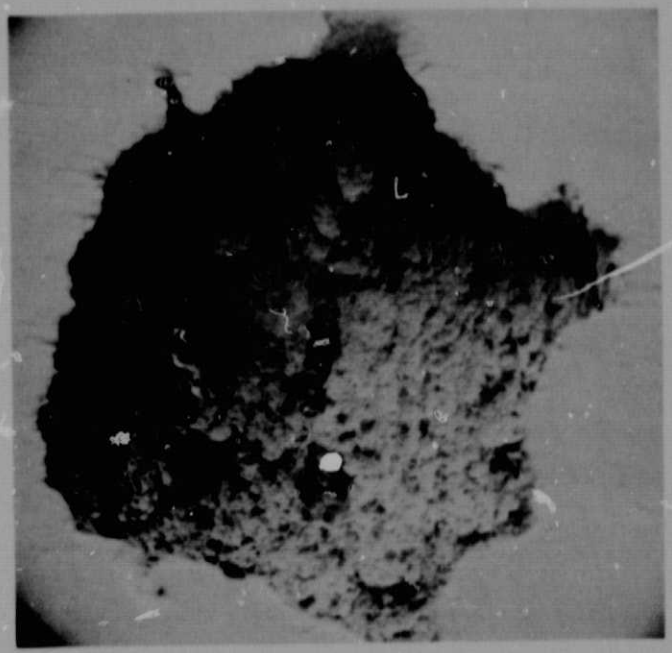

Fig. 5 - SEM micrographs of the interior surface of a sectioned bubble at various magnifications, (a) through (d).

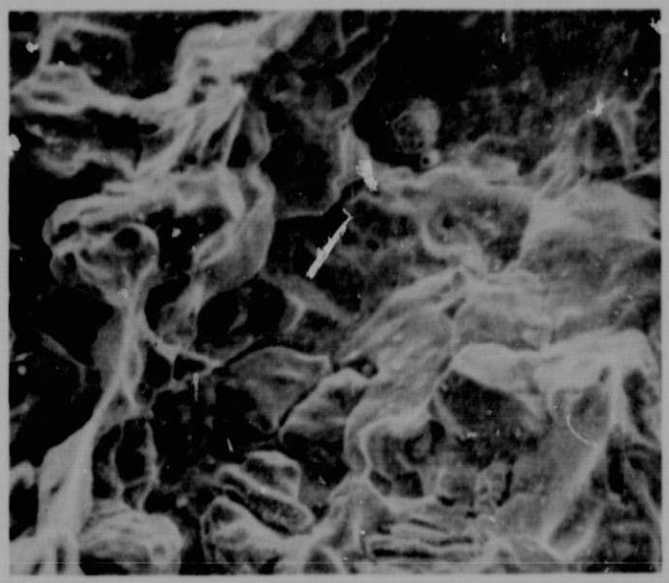

(c)

⊢15 μm⊣

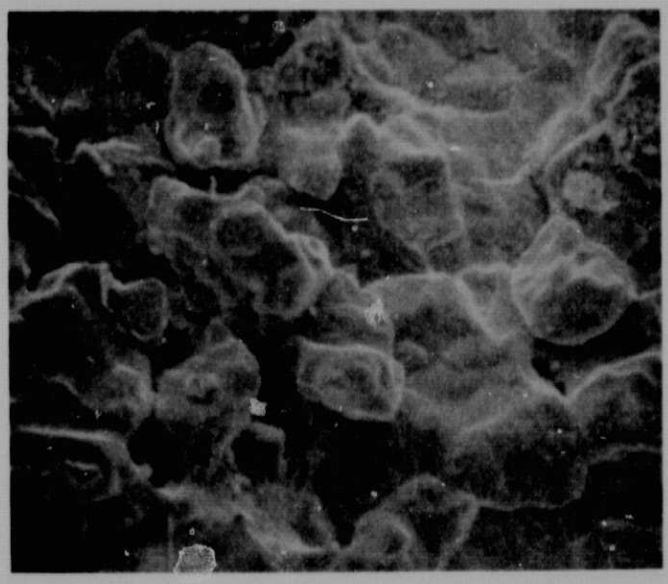

(d)

⊢10 μm⊣

Fig. 5 - Concluded.

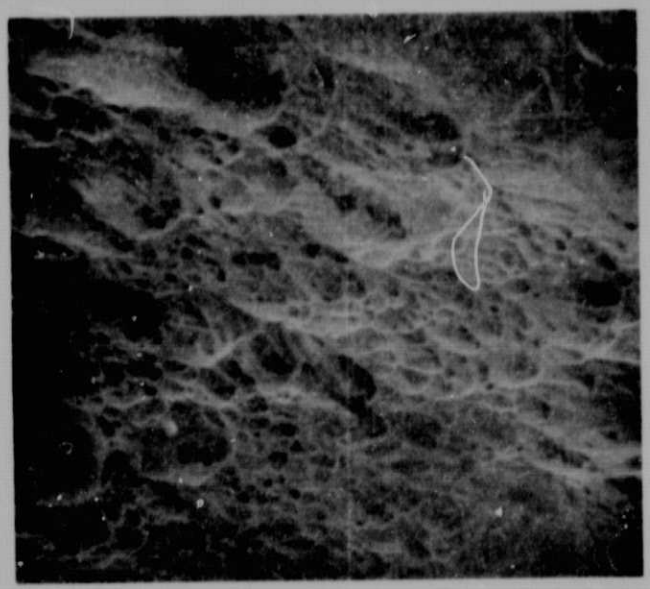

(a) *Specimen exposed to vacuum environment.*

(b) Specimen exposed to hydrogen environment showing intergranular separation and dimples.

(c) *Specimen exposed to hydrogen environment showing cleavage.*

Fig. 6 - Typical SEM fractographs of specimens.